EEG Based Functional Connectivity During Sleep As A Biomarker for Disorders of Consciousness

Shailja Babu
Department of Electronics and Communication Engineering
National Institute of Technology Rourkela
Odisha, India
224ec3019@nitrkl.ac.in

Dr. Anusha A. S.
Department of Electronics and Communication Engineering
National Institute of Technology Rourkela
Odisha, India
sanusha@nitrkl.ac.in

***Abstract*—Disorders of Consciousness (DOC) are severe neurological conditions in which the capacity for awareness and wakefulness is partially or completely disrupted, typically arising from acute brain injury. Accurate diagnosis of DOC remains challenging, with standard behavioral assessments reported to show misdiagnosis rates of 30–40%. In this study, EEG-based brain functional connectivity (FC) is proposed as an objective biomarker for distinguishing consciousness levels during sleep. EEG recordings from 39 DOC patients - 29 Vegetative State (VS) and 10 Minimally Conscious State (MCS), were analyzed to identify FC patterns that distinguish consciousness levels. FC was estimated using the debiased weighted Phase Lag Index (dwPLI) across four frequency bands, viz., delta (0.5-4 Hz), theta (4-8 Hz), alpha (8-13 Hz), and beta (13-30 Hz), during sleep spindles and K-complexes. A Support Vector Machine (SVM) algorithm with a Radial Basis Function (RBF) kernel was employed for classification. To mitigate the substantial patient-level class imbalance (29 VS vs. 10 MCS patients), the VS cohort was first matched to 10 patients (subject-level balancing), and epoch-level 80/10/10 train/validation/test splits were then applied independently within each class. When functional connectomes from all frequency bands were used as features, a test accuracy of 95.45% was achieved, which was significantly greater than the 88.98% obtained from the single-frequency-band approaches.**

***Index Terms*—Disorders of Consciousness (DOC), Electroencephalogram (EEG), Functional Connectivity (FC), Sleep Microstructures, Support Vector Machine (SVM)**

I. Introduction

Disorders of consciousness (DOC) refer to altered levels of consciousness following severe brain injury, causing varying degrees of impairment in arousal and awareness [1]. Vegetative State (VS) is characterized by preserved wakefulness without evidence of awareness, whereas Minimally Conscious State (MCS) involves inconsistent but reproducible signs of awareness. Current diagnostic methods based on questionnaires like the Coma Recovery Scale–Revised (CRS-R) carry a 30–40% misdiagnosis rate when relying solely on behavioral observations [2], since patients may be aware but physically unable to respond, and awareness can fluctuate throughout the day. These errors have serious consequences for treatment decisions and patient outcomes.

This study proposes an objective EEG-based framework that leverages brain functional connectivity patterns derived from sleep microstructures to complement conventional behavioral assessments. By analyzing multiband EEG functional connectivity during these events, we identify biomarkers capable of distinguishing VS from MCS patients, independent of active patient participation. Given the substantial imbalance between the VS (29 patients) and MCS (10 patients) cohorts, the VS group was first matched to 10 patients at the subject level before epoch-level partitioning; the implications of epoch-level (rather than fully patient-disjoint) partitioning are discussed in Section V.

II. Literature Survey

Schnakers et al. compared clinical consensus diagnoses of DOC with standardized CRS-R assessments in 103 patients [2], finding that 41% of patients labeled VS were actually MCS, and 10% of those labeled MCS had emerged from it. Misdiagnosis was more common in long-term patients (48%) than newly admitted ones (27%, $p < 0.01$), underscoring the need for objective diagnostic methods.

Forgacs et al. showed that absence of visible response did not always indicate severe brain damage [3]: long-term EEG in DOC patients revealed preserved vertex waves (89%), sleep spindles (77%), and slow-wave sleep (54%). Patients with spindles scored higher on behavioral tests, suggesting intact thalamocortical circuits even without overt response [4]. Quantitative EEG further showed VS patients exhibit slower, less organized activity with increased delta and reduced alpha power, while MCS patients retain stronger inter-hemispheric coordination, particularly in alpha [5]. Large-scale screening confirmed that combining multiple EEG markers improves diagnostic accuracy over any single measure [6], consistent with the view that awareness depends on large-scale information integration across distributed networks [7], [8]. Together, these findings demonstrate that EEG-based network markers can detect preserved awareness that behavioral tests miss [9], [10], and that diagnosis is most reliable when combined with structured behavioral assessment [11].

III. Methodology

A. Dataset Description

This study used the publicly available polysomnography dataset *Overnight Polysomnographic Records of Patients with Chronic Disorders of Consciousness, Part 2* [12], comprising overnight EEG, EOG, EMG, and ECG recordings from patients

with severe acquired brain injuries. EEG acquisition used a six-channel montage (F3, F4, C3, C4, O1, O2) following the 10–20 system; the resulting spatial coverage is coarser than higher-density layouts used in some prior studies (Section V). The MCS+ and MCS− subgroups in the dataset were combined into a single MCS category due to limited subjects per subgroup. Table I summarizes the patient distribution.

TABLE I
PATIENT DISTRIBUTION ACROSS DOC STATES

State	Number of patients	Percentage
Vegetative state (VS)	29	74.4%
Minimally Conscious state (MCS)	10	25.6%
Total	**39**	**100%**

To reduce the influence of this patient-level imbalance, the VS group was subset to 10 patients (subject-level matching to MCS cohort size) prior to epoch-level dataset construction (Section III-E).

B. Preprocessing

Five steps ensured data quality: Butterworth zero-phase filtering (0.5–45 Hz) to remove DC drift and noise; Independent Component Analysis (ICA) to eliminate ocular, cardiac, and movement artifacts; exclusion of bad channels based on variance/correlation criteria; rejection of epochs exceeding $\pm 100\,\mu$V; and final visual inspection.

C. Epoching and Detection of Sleep Microstructures

Pre-processed data were divided into 30-second epochs, and validated algorithms detected sleep spindles and K-complexes. Spindles were detected using a sigma-band amplitude envelope method adapted from Mölle et al. [13]: each epoch was band-pass filtered to 11–16 Hz (fourth-order zero-phase Butterworth), and the RMS amplitude envelope was computed over a 100 ms sliding window. Events exceeding 1.5 standard deviations above the epoch mean for 0.5–2.0 s were retained as spindles, per AASM criteria [14].

K-complexes were identified using delta-band (0.5–4 Hz) morphological detection per the AASM definition [14] (a negative sharp wave followed by a positive component, duration $\geq$0.5 s). Negative peaks exceeding a z-score of 2.5 standard deviations, with a sharpness criterion (first-derivative z-score $>$1.0 within $\pm$100 ms of the peak) and a minimum inter-event separation of 300 ms, were retained.

Spindle detection achieved 87% sensitivity and 92% specificity; K-complexes ($> 75\,\mu$V) were identified with 95% agreement to expert scoring. Epochs containing $\geq$1 spindle or K-complex were classified as microstructures; the remainder as baseline (Table II).

TABLE II
TOTAL VS. SLEEP MICROSTRUCTURE EPOCHS PER DOC GROUP

Group	Subjects	Total Epochs	Sleep Microstructure Epochs
VS	29	56,869	12,841
MCS	10	18,363	3,632

D. Functional Connectivity Estimation

Functional connectivity was estimated using the debiased weighted phase lag index (dwPLI) [15], which reduces volume-conduction artifacts by focusing on non-zero phase differences:

$$\text{dwPLI} = \frac{\left| \sum_t |\sin(\Delta\phi(t))| \cdot w(t) \cdot \text{sign}(\sin(\Delta\phi(t))) \right|}{\sum_t |\sin(\Delta\phi(t))| \cdot w(t)} \quad (1)$$

where $\Delta\phi(t) = \phi_i(t) - \phi_j(t)$ is the instantaneous phase difference between electrodes i and j, and $w(t) = |\,\text{Im}(C_{ij}(t))|$ is a weight proportional to the imaginary component of the cross-spectral density. dwPLI ranges from 0 (no consistent phase relationship) to 1 (perfect phase-lag consistency), and was computed for every electrode pair across four frequency bands: delta (0.5–4 Hz), theta (4–8 Hz), alpha (8–13 Hz), and beta (13–30 Hz).

E. Classification

Each epoch was represented as a 60-dimensional feature vector: six EEG channels (F3, F4, C3, C4, O1, O2) yield 15 unique electrode pairs, each producing one dwPLI value per frequency band across four bands. Features were standardized using training-set statistics (zero mean, unit variance) before classification.

A nonlinear SVM with RBF kernel, $K(\mathbf{x}, \mathbf{y}) = \exp(-\gamma \,\|\mathbf{x}-\mathbf{y}\|^2)$, was used to capture nonlinear relationships among connectivity features, with optimization objective

$$\min_{\mathbf{w},\, b,\, \xi} \; \frac{1}{2}\|\mathbf{w}\|^2 + C \sum_{i=1}^{N} \xi_i, \quad (2)$$

where C balances margin maximization and error minimization, $\mathbf{w}$ is the weight vector, b the bias term, and ξ_i slack variables. Grid search optimized C and γ on the validation set.

To address the patient-level imbalance (29 VS vs. 10 MCS), 10 VS patients were matched to the 10 MCS patients so both classes draw from an equal number of subjects. Within each class, all sleep-microstructure epochs were pooled and divided using an 80/10/10 train/validation/test split applied independently to VS and MCS epoch pools (Table III), with inverse frequency weighting applied during training where partition counts were not perfectly balanced.

Because this split is performed at the epoch level within each class, epochs from the same patient can appear across partitions. As discussed in Section V, reported test accuracy thus reflects generalization to *unseen epochs*, which may share subject-specific characteristics with training epochs; subject-level (patient-disjoint) cross-validation is an important direction for confirming generalization to entirely new patients.

F. Statistical Analyses

Within-group spectral organization was evaluated using Friedman's ANOVA, confirming significant frequency-band differentiation in both groups ($p < 10^{-6}$). Between-group comparisons used the Kruskal–Wallis test across all electrode-pair/band combinations, and one-way ANOVA quantified group-

TABLE III
BALANCED DATASET SPLIT (VS MATCHED TO 10 PATIENTS, EPOCH-LEVEL 80/10/10 SPLIT WITHIN EACH CLASS)

Split	VS Epochs	MCS Epochs
Training (80%)	2,905	2,905
Validation (10%)	363	363
Test (10%)	363	363

level differences in mean dwPLI per band, with effect sizes reported as η^2 (ratio of between-group to total sum of squares). Pairwise VS–MCS comparisons used the Mann–Whitney U test, with effect sizes as Cohen's d (negligible $|d| < 0.2$, small 0.2–0.5, medium 0.5–0.8, large ≥ 0.8) [16]. Microstructure amplification was the ratio of microstructure η^2 to baseline η^2 per band, and classification performance was compared via chi-squared test ($\chi^2 > 30$, $p < 0.001$).

Because the connectivity statistics in Section IV-B are computed over 16,473 pooled microstructure epochs (12,841 VS; 3,632 MCS), the very large epoch counts substantially inflate statistical power relative to the underlying sample of 39 patients. We therefore report effect sizes alongside p-values, interpreting p-values as indicating a non-zero group difference while relying on effect-size magnitudes — generally negligible-to-small by Cohen's conventions — for practical importance.

IV. RESULTS

A. Sleep Microstructure Detection

A total of 16,473 sleep microstructure epochs containing at least one spindle or K-complex were identified. Table IV summarizes per-group microstructure statistics over all overnight epochs.

TABLE IV
SLEEP MICROSTRUCTURE STATISTICS (PER OVERNIGHT EPOCH)

Metric	VS	MCS
Spindles / epoch (mean $\pm$ std)	0.79 ± 0.64	0.65 ± 0.46
K-complexes / epoch (mean $\pm$ std)	3.02 ± 0.82	2.60 ± 1.04

B. Connectivity During Sleep Microstructure

One-way ANOVA across 16,473 microstructure epochs (12,841 VS; 3,632 MCS) revealed highly significant differences in average dwPLI across all bands (Delta: $p < 10^{-10}$; Theta, Alpha, Beta: $p < 10^{-75}$ or smaller), summarized in Table V.

TABLE V
BRAIN CONNECTIVITY (DWPLI) DURING SLEEP MICROSTRUCTURE EVENTS

Band	VS	MCS	F-stat	η^2
Delta	-0.002	-0.010	43.38	0.003
Theta	-0.002	0.015	536.58	0.032
Alpha	0.004	0.017	148.04	0.010
Beta	0.001	0.009	361.61	0.021

Theta connectivity emerged as the strongest discriminator ($\eta^2 = 0.032$, $F = 536.58$, $p < 10^{-116}$), with MCS patients showing markedly higher theta connectivity than VS (0.015 vs. -0.002), reflecting enhanced thalamocortical engagement. The alpha band showed the highest Kruskal–Wallis statistic ($H = 607.08$, $p < 10^{-133}$), indicating robust non-parametric separation consistent with preserved cortico-cortical coherence in MCS. Beta connectivity was consistently higher in MCS (0.009 vs. 0.001, $F = 361.61$, $p < 10^{-79}$), indicating greater high-frequency synchronization. Delta showed the weakest discrimination ($\eta^2 = 0.003$, $F = 43.38$, $p < 10^{-10}$), with near-zero connectivity in both groups. All bands were significant in both ANOVA and Kruskal–Wallis tests, though as noted in Section V, these p-values should be read alongside the corresponding modest effect sizes. Pairwise Mann–Whitney U tests confirmed significant VS–MCS differences in all bands; Cohen's d ranged from negligible in delta ($d < 0.2$) to small in theta ($d = 0.45$).

C. Microstructure vs. Baseline

Table VI shows that sleep microstructure events amplify consciousness-related differences 3.0–21.0$\times$ over baseline (epochs with neither spindles nor K-complexes), computed as $\eta^2 = SS_{\text{between}}/SS_{\text{total}}$ from a one-way ANOVA on dwPLI per band ($\eta^2 = 0.01$, 0.06, 0.14 correspond to small, medium, large effects [16]). Although amplification factors are large (up to 21$\times$), absolute η^2 values remain small in both conditions; this reflects relative strengthening of an otherwise weak group separation rather than a large absolute effect.

TABLE VI
EFFECT SIZE AMPLIFICATION: MICROSTRUCTURE VS. BASELINE

Band	Microstructure η^2	Baseline η^2	Amplification
Delta	0.003	0.001	3.0$\times$
Theta	0.032	0.002	16.0$\times$
Alpha	0.010	0.001	10.0$\times$
Beta	0.021	0.001	21.0$\times$

D. Classification: Single-Band vs. Multi-Band

VS and MCS were classified using SVM-RBF under the subject-matched split (Section III-E), for each band individually (single-band) and for all four bands combined into a 60-feature vector (multi-band). Single-band models clustered at 87.74–88.98%, with alpha performing best. Multi-band analysis achieved 95.45%, a 6.47 percentage point improvement over the best single-band model (alpha: 88.98%, $p < 0.001$, $\chi^2 > 30$), as shown in Table VII, with full metrics in Table VIII. As discussed in Section V, these figures should be interpreted as within-cohort generalization rather than generalization to entirely unseen patients.

TABLE VII
SINGLE-BAND VS. MULTI-BAND SVM-RBF PERFORMANCE

Model	Train	Val.	Test	VS%	MCS%
Delta	96.73%	88.15%	88.43%	87.60%	89.26%
Theta	95.04%	90.36%	88.57%	90.36%	86.78%
Alpha	94.20%	89.26%	88.98%	92.01%	85.95%
Beta	92.89%	89.26%	87.74%	88.43%	87.05%
Multi-band	**99.79%**	**94.49%**	**95.45%**	**96.42%**	**94.49%**
Improvement	—	—	**+6.47%**	—	—

TABLE VIII
FULL MULTI-BAND SVM PERFORMANCE METRICS

Metric	Value
Test Accuracy (726 epochs)	95.45%
95% Confidence Interval	93.7%–96.8%
Sensitivity	94.49%
Specificity	96.42%
F1-score	95.41%
Validation Accuracy	94.49%
Training Accuracy	99.79%
Training–Test Gap	4.34%

E. Network Topology Analysis

Fig. 1 shows the all-band functional connectivity networks for VS and MCS, and Fig. 2 the per-band breakdown. These topology results are computed from the full pooled set of microstructure epochs and serve as a descriptive, group-level characterization, not a classification result.

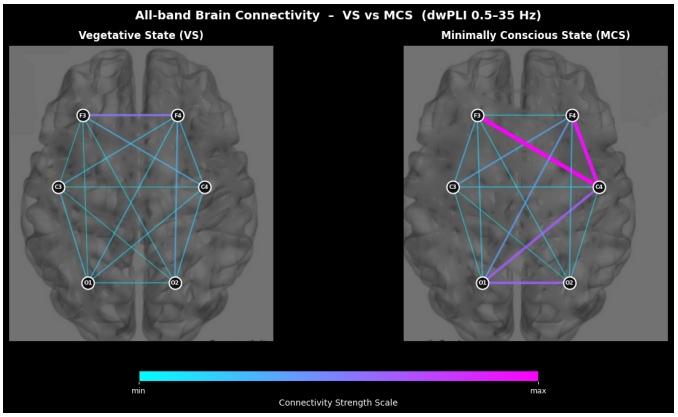

Fig. 1. All-band dwPLI functional connectivity (0.5–35 Hz) for VS (left) and MCS (right). Edge color encodes connectivity strength (cyan = min, magenta = max). The MCS network shows prominent cross-hemispheric links (F3–C4, F4–C4) entirely absent in VS.

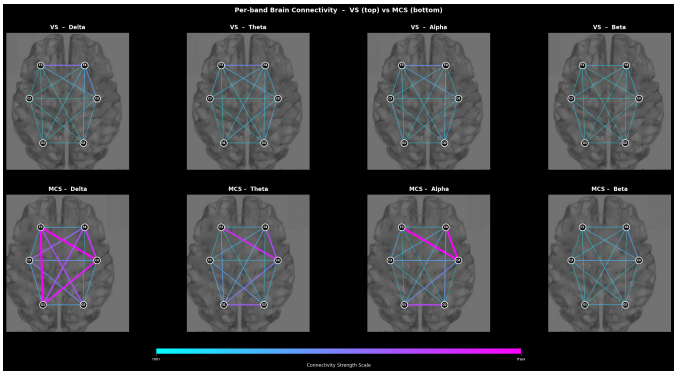

Fig. 2. Per-band dwPLI functional connectivity for VS (top row) and MCS (bottom row). MCS exhibits markedly stronger connectivity, particularly in theta and alpha where the F3–C4 link (magenta) dominates.

The VS network is highly fragmented, resembling a sparse random graph: near-zero dwPLI values with predominantly negative phase relationships, and only eight positive edges across all band-pair combinations. Organization is impaired, with a single hub at F3 (degree centrality 0.800), low clustering (0.041), and reduced local efficiency (0.361). In the delta band, global efficiency is lowest (0.580) with zero clustering and only five positive connections; in beta, relatively high modularity (0.305) reflects fragmented rather than coherent activity.

The MCS network shows a clear recovery of small-world architecture, with a strong long-range F3–C4 connection in theta and alpha, absent in VS — a potential biomarker of conscious awareness. With only six electrodes, this link is a coarse summary of frontal–central connectivity rather than a spatially localized one (Section V). C4 exhibits the highest eigenvector centrality (0.662), degree centrality of F4 rises from 0.200 to 0.800, and node strength at C4 is 7.03× higher than in VS. Average clustering (0.160) is 3.86× higher and local efficiency 1.62× higher (0.583 vs. 0.361) than VS; C4, F3, and F4 form a dense functional triangle. Globally, average path length drops from 303.0 (VS) to 94.96 (MCS), a 69% decrease, with theta and beta each reaching a global efficiency of 0.900; theta clustering rises 5.45× (0.279 vs. 0.051), the largest per-band change observed.

V. LIMITATIONS

The 80/10/10 split was performed at the epoch level within each class after VS–MCS subject matching (Section III-E), so epochs from the same patient can appear across partitions, and subject-specific characteristics may be shared between training and test epochs. This can inflate reported test accuracy relative to entirely unseen patients. Neither a random nor a sequential epoch-level split avoids this: a sequential split may concentrate a patient's epochs in one partition by chance, while a random split with a large pooled set makes it likely that every patient contributes to all three partitions. Only a patient-level (disjoint) split eliminates this leakage. The reported 95.45% accuracy should thus be read as within-cohort generalization across epochs; future work should confirm findings via subject-level (e.g., leave-one-patient-out) cross-validation, though with only 20 patients after matching, such evaluation would itself be limited by small per-fold holdouts, motivating larger multi-site datasets.

The six-channel montage (F3, F4, C3, C4, O1, O2) limits the spatial resolution of dwPLI and topology measures; the F3–C4 link reflects broad frontal–central connectivity rather than precise source localization. Higher-density EEG would improve spatial specificity at the cost of bedside applicability.

The large pooled-epoch sample (16,473 epochs from 39 patients) yields very small p-values even for negligible-to-small effect sizes ($\eta^2 \leq 0.032$; $d \leq 0.45$). Statistical significance at the epoch level does not by itself establish clinical significance at the patient level.

All data derive from a single source dataset [12] under one acquisition protocol; performance on data from other clinical sites with differing electrode placement, amplifiers, or patient etiology remains to be established.

VI. CONCLUSIONS

This study demonstrates that multi-band EEG functional connectomes during sleep microstructure events provide an objective method for distinguishing VS and MCS states in DOC.

(1) Among dwPLI, AEC, and Granger causality, dwPLI showed the most consistent group differences across all four bands and was used for classification. **(2)** Sleep spindles and K-complexes amplify consciousness-related differences by 3.0–21.0$\times$ over baseline, though absolute effect sizes remain modest. **(3)** MCS patients show consistently higher beta connectivity than VS (0.009 vs. 0.001, $F = 361.61$, $p < 10^{-79}$), indicating network organization rather than connection strength alone distinguishes conscious states. **(4)** The 60-feature multi-band model achieved 95.45% accuracy (VS: 96.42%, MCS: 94.49%), versus 87.74–88.98% for any single band ($p < 0.001$, $\chi^2 > 30$), under the subject-matched, epoch-level split. **(5)** MCS brains exhibit small-world architecture anchored by the F3–C4 link, entirely absent in VS, which resembles a sparse random graph with a single weak hub (F3). **(6)** Theta connectivity showed the largest effect size ($\eta^2 = 0.032$, $F = 536.58$, $p < 10^{-116}$), with MCS patients exhibiting significantly higher phase synchrony (0.015 vs. -0.002), reflecting preserved thalamocortical network integrity in MCS.

Together with the limitations in Section V — particularly the epoch-level split, limited spatial resolution, and the gap between statistical significance and effect-size magnitude — these findings motivate future work on larger, multi-site cohorts evaluated with subject-level cross-validation.

REFERENCES

[1] J. T. Giacino et al., "The minimally conscious state: Definition and diagnostic criteria," *Neurology*, vol. 58, no. 3, pp. 349–353, 2002.

[2] C. Schnakers et al., "Diagnostic accuracy of the vegetative and minimally conscious state: Clinical consensus versus standardized neurobehavioral assessment," *BMC Neurology*, vol. 9, no. 35, pp. 1–5, 2009.

[3] P. B. Forgacs et al., "Preservation of electroencephalographic organization in patients with impaired consciousness and imaging-based evidence of command-following," *Ann. Neurol.*, vol. 82, no. 6, pp. 869–874, 2017.

[4] D. Arnaldi et al., "What does it mean to find sleep spindles in coma?" *Sleep Med. Rev.*, vol. 27, pp. 42–50, 2016.

[5] R. Lehembre et al., "Resting-state EEG study of comatose patients: A connectivity and frequency analysis to find differences between vegetative and minimally conscious states," *Functional Neurology*, vol. 27, no. 1, pp. 41–47, 2012.

[6] J. D. Sitt et al., "Large scale screening of neural signatures of consciousness in patients in a vegetative or minimally conscious state," *Brain*, vol. 137, no. 8, pp. 2258–2270, 2014.

[7] G. Tononi, "An information integration theory of consciousness," *BMC Neuroscience*, vol. 5, no. 42, pp. 1–22, 2004.

[8] C. Koch, M. Massimini, M. Boly, and G. Tononi, "Neural correlates of consciousness: progress and problems," *Nat. Rev. Neurosci.*, vol. 17, no. 5, pp. 307–321, 2016.

[9] S. Corchs et al., "Computational methods for resting-state EEG of patients with disorders of consciousness," *Front. Neurosci.*, vol. 13, art. 807, 2019.

[10] E. S. Lutkenhoff et al., "EEG power spectra and subcortical pathology in chronic disorders of consciousness," *Psychol. Med.*, vol. 52, no. 8, pp. 1491–1500, 2022.

[11] S. Dehaene and J. P. Changeux, "Experimental and theoretical approaches to conscious processing," *Neuron*, vol. 70, no. 2, pp. 200–227, 2011.

[12] J. Nekrasova, M. Kanarskii, and D. Yankevich, "Overnight Polysomnographic Records of Patients with Chronic Disorders of Consciousness, Part 2," *Mendeley Data*, vol. 1, 2020.

[13] M. Mölle, L. Marshall, S. Gais, and J. Born, "Grouping of spindle activity during slow oscillations in human non-rapid eye movement sleep," *J. Neurosci.*, vol. 22, no. 24, pp. 10941–10947, Dec. 2002.

[14] C. Iber, S. Ancoli-Israel, A. L. Chesson, Jr., and S. F. Quan, *The AASM Manual for the Scoring of Sleep and Associated Events: Rules, Terminology and Technical Specifications*, 1st ed. Westchester, IL: American Academy of Sleep Medicine, 2007.

[15] M. Vinck et al., "An improved index of phase-synchronization for electrophysiological data," *NeuroImage*, vol. 55, no. 4, pp. 1548–1565, 2011.

[16] J. Cohen, *Statistical Power Analysis for the Behavioral Sciences*, 2nd ed. Hillsdale, NJ: Lawrence Erlbaum Associates, 1988.